Research Article

The combined influences of heat transfer, compliant wall properties and slip conditions on the peristaltic flow through tube

I. M. Eldesoky[1,2] · R. M. Abumandour[1] · M. H. Kamel[3,4] · E. T. Abdelwahab[1]

Abstract
In this research, the peristaltic flow with heat transfer through the two-dimensional horizontal tube of compliant wall properties with slip at boundaries is analyzed analytically. An approximated theoretical model is constructed of spring-backed flexible compliant walls pipe, chosen to move as sinusoidal wave. Perturbation solution of the governing equations is obtained with small parameter ε, which means the amplitude ratio, and defined as the ratio of wave amplitude divided by tube radius. The influence of several parameters of slip conditions, wall properties and heat transfer on the dynamics of the liquid through the tube is mathematically studied, resulting in relations describing the fluid flow behavior and the induced net flow rate under the various values of flow parameters as "liquid compressibility, slip flow factor, and wave number", heat transfer parameter like Prandtl number, and elastic wall parameters such as "wall tension, wall damping coefficient, wall stiffness, and wall rigidity". Graphs for net flow rate under the effect of pervious parameters are plotted. Results disclose that the parameters of tube wall features, compressibility of liquid, Knudsen number for wall slip, and heat transfer in the presence of peristaltic pumping have a significant effect on net flow rate induced. This research has numerous related applications in different branches of science such as biological studies for blood flow motion in living creatures and also in industry including simulation of induced elastic waves for fluid flow through a tube.

Keywords Peristaltic · Wall properties · Heat transfer · Slip conditions

List of symbols

R	Tube mean radius
$\vec{V}$	The fluid velocity vector
Φ	Viscous dissipation rate
p	The fluid pressure
ρ	The fluid density
z	The coordinate in the stream wise direction
r	The coordinate normal to the flow direction
t	The time
v_r	The radial velocity
v_z	The velocity in the flow direction
μ	The fluid dynamic viscosity coefficient
T	The fluid temperature
K_t	The thermal conductivity
K^*	The liquid compressibility factor
ρ_o	The standard density corresponding to reference pressure p_c
$\eta(x,t)$	The vertical wall displacement
a	The wave amplitude
λ	The wavelength
c	The wave speed
$L(\eta)$	The compliant wall differential operator
T	Longitudinal tension per unit width of wall
m	Mass per unit area
D	Damping factor
B	Wall bending coefficient
K	Spring stiffness
p_o	The external pressure acting on the boundary

✉ I. M. Eldesoky, eldesokyi@yahoo.com | [1]Basic Engineering Sciences Department, Faculty of Engineering, Menofia University, Shebin El-Kom, Egypt. [2]Basic Engineering Sciences Department, Elmenofia Higher Institute of Engineering and Technology, El-Menofia, Egypt. [3]Department of Engineering Mathematics and Physics, Faculty of Engineering, Cairo University, Giza, Egypt. [4]Dean of El-Madina Higher Institute of Engineering and Technology, Giza, Egypt.

SN Applied Sciences (2019) 1:897 | https://doi.org/10.1007/s42452-019-0915-4

Received: 8 April 2019 / Accepted: 11 July 2019 / Published online: 22 July 2019

A	Mean free path of molecules
R_e	Reynolds number
T_o	The mean fluid temperature
T_1	The uniform temperature
χ	The compressibility number
α	The wave number
P_r	Prandtl number
E	Eckert number
B_r	Brinkman number
c_p	The specific heat at constant pressure
ε	The amplitude ratio
Kn	Knudsen number
υ_o	Kinematic viscosity
I_o	The modified Bessel function of first kind zero order
I_1	The modified Bessel function of first kind first order
$\langle V_z(r) \rangle$	The mean time axial velocity
$\langle Q \rangle$	The net axial flow rate

1 Introduction

It is a fact to mention that the analysis for the transport of biofluids through the peristaltic mechanism draws the physiologists' attention in their investigations due to ongoing growth in the biomedical and technological applications related to this type of motion. In the beginning, it is relevant to understand the nature of the peristaltic flow and how it is formed. Fluid locomotion along the path of this mechanism occurs as a result of the dilatation and constriction of tube/channel wall due to the elastic wall properties. In the biological systems, peristalsis is a natural process which is familiar and occurring inside the living bodies such as the urine flow through the ureter from kidney to the bladder, the movement of intestines, gastrointestinal, bile tubes, and many glandular conduits. Peristaltic activity appears also in the motion through the small blood vessels. The esophagus is elastic muscular tube resulting in peristalsis waves causing propulsion of the food bolus towards the stomach. Sperm are locomoted along the vas deferens by the peristaltic contractions. The uterine tubes are the female muscular passages which use the peristalsis action to move the ova to the uterus. Peristalsis causes the movement of lymph through lymphatic tract. Also it is used in biomedical machines as heart lung pump which helps to pump the blood. By applying the principles of peristalsis in industry, mechanical finger and roller pumps were manufactured for transporting the corrosive and toxic fluids to avoid any further damage. Introducing heat transfer is very necessary in many medical processes like dialysis treatment and oxygenation. Heat transfer effect is clearly significant in the treatment of cancer cells. Slip phenomenon occurring at the walls exist in the case of pumping rarefied gasses and the flow of polymers. Literature review for the experimental and theoretical studies handling the peristaltic action and heat transfer influence and its importance is introduced as follows.

In the beginning, Latham [1] performed a number of experimental studies using simple geometry of plastic tube taking the shape of peristalsis by neglecting the longitudinal motions of the tube walls and axisymmetric models and then compared the results with that obtained from the theoretical analysis in which long wave length and zero Reynolds number were assumed for the two-dimensional sinusoidal wave shaped tube. After that, Burns and Parkes [2] introduced the axisymmetric models of pipes and wavy shaped symmetrical channel for Stokes flow with small Reynolds number. Shapiro [3] presented theoretical analysis for the peristaltic wave to obtain relations for flow rate and pressure gradient for Poiseuille flow. Shapiro et al. [4] used the long wave length approximation with low Reynolds number to obtain calculation for the net flow rate resulting from the peristaltic waves and two physiological phenomena appeared, one is known as "reflux" and the other called "trapping". Fung and Yih [5] verified the analysis of [3]. Srivastava and Srivastava [6–9] analyzed the peristaltic transport for different theoretical models and applications of human body such as vas deferens, small intestines, and reproductive tract. Hina et al. [10] have discussed the peristaltic motion of shear-thinning and shear-thickening fluids by considering the elastic properties of the curved channel walls using the regular perturbation method for the analytical analysis. Hina et al. [11] have introduced heat and mass transfer in the presence of viscous dissipation and thermophoresis effects on the peristaltic flow of Powell–Eyring fluid through curved passage with complaint walls by using perturbation technique with long wavelength and low Reynolds number and the results disclosed that, the material parameters of the Powell–Eyring fluid have a strong effect on the flow field. Makinde et al. [12] analyzed the combined effects of magnetic field, thermal radiation, heat source, velocity slip and thermal jump on peristaltic transport of an electrically conducting Walters-B fluid through a compliant walled channel with the aid of perturbation method and it was found that, the velocity distribution was decreased while the fluid temperature raised by the increase in Hartmann number, and also the trapping bolus was increased by increasing the magnetic parameter. Bhatti and Zeeshan [13] have investigated the particle concentration for the two phase flow besides the heat and mass transfer in the presence of fluid slip at the boundary for Casson fluid model moving peristaltically. They have used the analytical long wavelength technique and the results showed that

the particulate concentration and slip effects have a great impact on the velocity distribution. Eldesoky et al. [14] have analyzed the different influences of relaxation time, slip, elastic features for the flexible channel on the peristaltic motion of compressible fluid of Maxwellian model. Takabatake et al. [15] presented a numerical investigation for evaluation of the efficiency of the peristaltic propagation through circular passage. E. El-Shehawy et al. [16] studied the influence of wall slip on the wavy transport of non-Newtonian Maxwell liquid through rectangular channel.. Kamel et al. [17] have studied the combined effects of wall slip and suspension concentration on the peristaltic wave. Tang and Rankin [18] presented the asymptotic and numerical and analysis for nonlinear peristaltic flow through flexible free boundaries. Heat transfer also participates in the studies related to the peristaltic transport. Shen and Ebel [19] analyzed the peristaltic process for heat conducting fluid using two different asymptotic techniques. Dar and Elangovan [20] discussed the influence of both heat and mass transfer and an inclined magnetic field on the peristaltic flow of a couple stress fluid moving in an inclined channel by using the methodology of long wavelength and low Reynolds number to obtain relation for temperature distribution, pressure rise and friction force under the effect of heat and magnetic field parameters. Abd-Alla et al. [21] investigated the various influences of space porosity, rotation, heat and mass transfer and compliant wall features on the peristaltic flow of an incompressible Newtonian fluid in a channel. Using long wavelength and low Reynolds number approximation, solutions were obtained for the stream function, temperature, concentration field, velocity and heat transfer coefficient and the pervious parameters have a strong effect on the dynamic flow behaviour. But Tang and Shen [22] analyzed the peristaltic mechanism in the existence of heat transfer and pressure drop occurring in flexible tube using Stokes and long wave techniques. The works [23, 24] analyzed the temperature distribution and heat coefficients effect on the wavy flow in the rectangular duct. Vajravelu et al. [25] used the long wave technique to analyze the heat transfer and space porosity for the wavy transport through concentric vertical tube. Vasudev et al. [26] discussed also the influence of the same heat and porosity parameters of [25] on the peristaltic flow through two-dimensional vertical channel. Mekheimer [27] studied the combined influences of transverse magnetic field and heat flow across the boundaries on the travelling wave of Newtonian liquid through vertical annuli tube. Nadeem et al. [28] investigated the heat transport process across a non-uniform tube carrying out Johnson Segalman fluid which was travelling peristaltically. The elastic wall properties have a strong effect on the wavy fluid flow behavior in terms of mean axial velocity, pressure, and the net flow rate. These wall properties were expressed as flexible wall model supported by elastic spring to dissipate the vertical wall displacement and wall damper to damp the normal wall velocity. Researches relevant to this type are presented in the following. Pandey and Chaube [29] investigated the influence of flexible wall features on the couple stress fluid travelling peristaltically. Hina et al. [30] investigation handled the wall properties impact on the wavy flow of Maxwellian liquid through duct. Radhakrishnamacharya and Srinivasulu [31] took both effects of wall properties and heat transfer on the peristaltic transport of fluid via channel in their study. Srinivas et al. [32] studied the influence of several variables of wall slip, magnetic field, wall properties, and heat transfer on the wavy flow through channel. Also Srinivas et al. [33] introduced the mass transfer and space porosity effects besides the variables of [32]. Eldabe and Abou-Zeid [34] obtained a solution for the temperature distribution and mean axial velocity for micropolar fluid peristaltic locomotion through tube under various parameters of viscoelastic wall. Hayat et al. [35] analyzed the action of wall features, heat parameters, permeability of porous area, and magnetic field parameter on the wavy motion of Maxwellian fluid. As the liquid compressibility has a significant effect on the nature of the fluid transport, then it draws the interest of many researchers. Anderson [36] presented the basics of compressible fluid. Aarts and Ooms [37] carried out the first try to investigate the transversal wavy pumping of compressible liquid using perturbation approach to obtain relation for calculation of the net flux; the results showed that the liquid compressibility has a strong effect on the resulting net flux. Acoustic source induced an ultrasound and its transport took a peristaltic shape and is used for improving oil extraction process from porous rock. Mekheimer and Abdel-Wahab [38] obtained expressions for mean axial velocity, net velocity at channel wall, and mean velocity perturbation function in terms of various flow and elastic wall parameters for the compressible fluid flow resulting from the surface acoustic wave in planar channel. Eldesoky et al. [39] analyzed both influences of liquid compressibility and suspension concentration on the wavy compressible flow via rectangular channel; the results showed that the increase in particle concentration causes an increase in the mean flow velocity, whereas the velocity profile was insensitive to the liquid compressibility. Elshehawey et al. [40] also analyzed the behaviour of aviscoelastic compressible liquid moving peristaltically via tapered pore. Eldesoky and Mousa [41, 42] presented investigations handling the peristaltic motion of compressible liquid in a tube and its relation to aerospace branch, then adding various parameters of relaxation time and porous area for Maxwellian model travelling through the tube in the second article. Eldesoky [43] added the wall slip influence to the other parameters

of [42] and the results showed that net flux was sensitive to slip coefficient, relaxation time, liquid compressibility, and Reynolds number.

To the best of the author's survey, it is noted that there is no previous attempt to study the combined influences of wall properties and slip conditions in the presence of heat transfer on the net flow rate resulting from the induced peristaltic wave through a horizontal tube. So that, the present study is the first attempt to combine the effects of heat transfer, wall slip and elastic wall properties on the peristaltic transport through tube in $(r - z)$ coordinates by using the analytical perturbation methodology. The motivation for this research is attempt to reach the best description approaching the real model for this kind of unsteady and oscillatory flow through tube. In the real systems, such types of motion occur due to muscle's contraction and expansion as a result of elastic feature for the walls. Then, it is a point of interest to analyze the characteristics of flexibility for compliant walls. The walls of the tube have elastic features which can deform and collapse causing the motion for the fluid and resulting in a change the dynamic behavior of the fluid flow. The flexible wall is modeled as a spring-backed plate-membrane-type wall to approach the real system. The plate-membrane wall executes motion purely perpendicular to the surface. And also, most of the fluid flow in the real systems can be treated as viscous flow, for instance, in case of blood flow through the arteries, the walls are subject to some degree of roughness. Interestingly, it is realistic to note that, the fluid flow can be treated as a continuous medium through micro-domains such as arteries and capillaries which are prone to constrictions for various pathological reasons. Eventually, introducing the heat transfer is beneficial in the treatment for some of diseases that affect the cardiovascular system, then the heat transfer will change the dynamic behaviour for the fluid flow, so that, it is important to add the heat transfer to understand the nature of fluid transport. The real application in biology appear obviously in the collapsible tubes in the critical positions in the living creatures such as the wavy transport in the veins above the heart, arteries under the cuff also, biological and engineering examples indicating the compliant wall action such as the pressure pulse propagation in the cerebrospinal fluid system and blood flow in cardiovascular system. The elastic properties of the collapsing tubes in the real physiological systems are related to the muscles effect. The former studies did not concentrate on the effects of compliant walls for the tube in presence of heat transfer for compressible flow.

Then, the main objective of the current study is to analyze the effect of various parameters of flexible wall such as "damping factor, wall tension, wall rigidity, and wall elasticity" in addition to the flow factors such as "liquid compressibility, slip coefficient, and Reynolds number" and heat transfer coefficients like Prandtl number on the net flow rate of the travelling wave. Perturbation approach with small amplitude is used for obtaining mathematical relations describing the mean axial velocity, the net flux, the liquid pressure, and the liquid temperature in terms of the pervious parameters. The zero-order pressure gradient is ignored and the zero-order temperature is supposed to be constant. The travelling fluid is compressible. The elastic wall model is constructed to take the form of spring-backed compliant walls.

2 Problem formulation

Suppose a model of an elastic sinusoidal wave of compressible viscoelastic liquid travelling through tube with mean radius R with compliance walls shown in Fig. 1. This propagating wave with small amplitude is considered to be peristaltic wave with spring-backed compliant walls.

The system of conservation equations (continuity, Navier–Stokes and energy, respectively) that govern the fluid flow in vector notation form, as following [44]:

$$\begin{aligned}
&\frac{\partial \rho}{\partial t} + \nabla \cdot (\rho \vec{V}) = 0 \\
&\rho \frac{\partial \vec{V}}{\partial t} + \rho(\vec{V} \cdot \nabla)\vec{V} = -\nabla P + \mu(\nabla^2 \vec{V}) + \frac{\mu}{3}\nabla(\nabla \cdot \vec{V}) \\
&\rho c_p \left[\frac{\partial T}{\partial t} + (\vec{V} \cdot \nabla)T\right] = (\nabla \cdot K_t \nabla T) + \Phi
\end{aligned} \tag{2.1}$$

Equation of state and its solution were introduced by Anderson [36] and Aarts and Ooms [40] as follows.

$$\begin{aligned}
&\frac{\partial \rho}{\partial p} = \rho k^* \\
&\rho = \rho_o e^{(k^*(p-p_c))}
\end{aligned} \tag{2.2}$$

Walls of channel are taken flexible with elastic features. This model is supposed to be spring-backed flexible walls model which allows only vertical displacement and horizontal deformation does not exist; thus the model is called compliant wall tube. Relation for $\eta(x, t)$ was obtained by [37] as follows:

$$\eta(z, t) = a \cos \frac{2\pi(z - ct)}{\lambda} \tag{2.3}$$

Equation for compliant wall properties is obtained as [38].

$$L(\eta) = p - p_o = -T\frac{\partial^2 \eta}{\partial z^2} + m\frac{\partial^2 \eta}{\partial t^2} + D\frac{\partial \eta}{\partial t} + B\frac{\partial^4 \eta}{\partial z^4} + K\eta \tag{2.4}$$

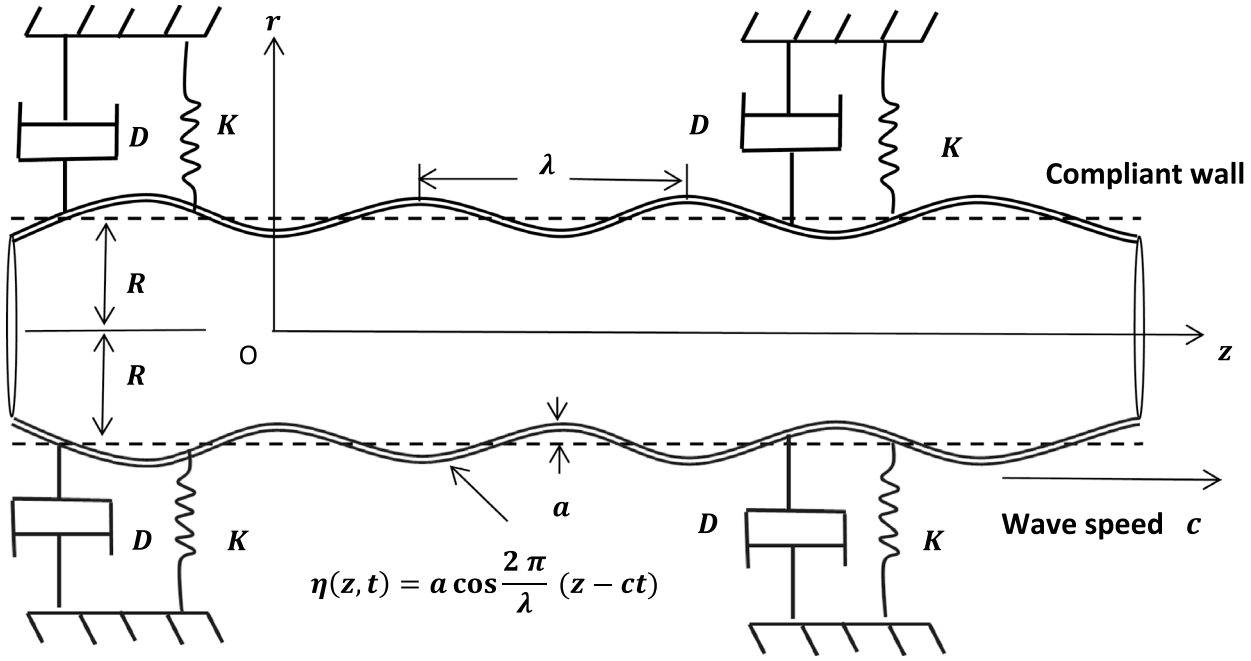

Fig. 1 Diagram of compliant wall tube model

2.1 Boundary conditions

The wavy transport exists under various conditions which occur at the tube walls. These conditions determine the flow behavior and are introduced at $r = (R + \eta)$ as follows:

- Slip and impermeability conditions associated with the fluid are

$$\left.\begin{aligned} v_z(r,z,t) &= A\frac{\partial v_z}{\partial r} \\ v_r(r,z,t) &= \frac{\partial \eta(z,t)}{\partial t} \end{aligned}\right\} \tag{2.5}$$

- The pressure gradient is affected by the nature of elastic wall so, it is introduced as follows:

$$\begin{aligned} \frac{\partial P}{\partial z} &= \frac{\partial}{\partial z}\left(m\frac{\partial^2\eta}{\partial t^2} + D\frac{\partial \eta}{\partial t} + B\frac{\partial^4\eta}{\partial x^4} - T\frac{\partial^2\eta}{\partial x^2} + K\eta\right) \\ &= \mu\left(\frac{\partial^2 v_z}{\partial r^2} + \frac{1}{r}\frac{\partial v_z}{\partial r} + \frac{\partial^2 v_z}{\partial z^2}\right) + \frac{\mu}{3}\frac{\partial}{\partial z}\left(\frac{\partial v_r}{\partial r} + \frac{v_r}{r} + \frac{\partial v_z}{\partial z}\right) \\ &\quad - \rho\left(\frac{\partial v_z}{\partial t} + v_r\frac{\partial v_z}{\partial r} + v_z\frac{\partial v_z}{\partial z}\right) \end{aligned} \tag{2.6}$$

- The wall temperature is oscillating about a nonzero mean temperature as [34] with the temperature at $r = 0$, the center of tube (case of symmetry) are described respectively, as:

$$\left.\begin{aligned} T &= T_1 + \frac{a}{R}(T_1 - T_o)cos\frac{2\pi}{\lambda}(z - t) \\ \frac{\partial T}{\partial r} &= 0 \end{aligned}\right\} \tag{2.7}$$

Introducing nondimensional analysis (2.7.1) for Eqs. (2.1), (2.2) and (2.5)–(2.7) then dropping over-bars, the pervious governing equations and boundary conditions can be rewritten in the following form:

$$\left.\begin{aligned} &\frac{\partial \rho}{\partial t} + v_r\frac{\partial \rho}{\partial r} + v_z\frac{\partial \rho}{\partial z} + \rho\left(\frac{\partial v_r}{\partial r} + \frac{v_r}{r} + \frac{\partial v_z}{\partial z}\right) = 0 \\ &\rho\frac{\partial v_r}{\partial t} + \rho\left(v_r\frac{\partial v_r}{\partial r} + v_z\frac{\partial v_r}{\partial z}\right) = -\frac{\partial p}{\partial r} \\ &\quad + \frac{1}{R_e}\left(\frac{\partial^2 v_r}{\partial r^2} + \frac{1}{r}\frac{\partial v_r}{\partial r} - \frac{v_r}{r^2} + \frac{\partial^2 v_r}{\partial z^2}\right) + \frac{1}{3R_e}\frac{\partial}{\partial r}\left(\frac{\partial v_r}{\partial r} + \frac{v_r}{r} + \frac{\partial v_z}{\partial z}\right) \\ &\rho\frac{\partial v_z}{\partial t} + \rho(v_r\frac{\partial v_z}{\partial r} + v_z\frac{\partial v_z}{\partial z}) = -\frac{\partial p}{\partial z} \\ &\quad + \frac{1}{R_e}\left(\frac{\partial^2 v_z}{\partial r^2} + \frac{1}{r}\frac{\partial v_z}{\partial r} + \frac{\partial^2 v_z}{\partial z^2}\right) + \frac{1}{3R_e}\frac{\partial}{\partial z}\left(\frac{\partial v_r}{\partial r} + \frac{v_r}{r} + \frac{\partial v_z}{\partial z}\right) \\ &\rho P_r R_e\left(\frac{\partial \theta}{\partial t} + v_r\frac{\partial \theta}{\partial r} + v_z\frac{\partial \theta}{\partial z}\right) = \frac{\partial^2\theta}{\partial r^2} + \frac{1}{r}\frac{\partial \theta}{\partial r} + \frac{\partial^2\theta}{\partial z^2} + B_r\left[\frac{\partial v_z}{\partial r} + \frac{\partial v_r}{\partial z}\right]^2 \\ &\quad + 2B_r\left[\left(\frac{\partial v_r}{\partial r}\right)^2 + \left(\frac{v_r}{r}\right)^2 + \left(\frac{\partial v_z}{\partial z}\right)^2\right] - \frac{2}{3}B_r\left[\frac{\partial v_r}{\partial r} + \frac{v_r}{r} + \frac{\partial v_z}{\partial z}\right]^2 \\ &\rho = e^{\chi(p-p_o)} \end{aligned}\right\} \tag{2.8}$$

- The boundary conditions at $r = (1 + \eta)$ are

$$\left.\begin{aligned} & v_z = kn\frac{\partial v_z}{\partial r},\ v_r = \frac{\partial \eta}{\partial t} \\ & \frac{\partial}{\partial z}\left(m\frac{\partial^2\eta}{\partial t^2} + \frac{D_w}{R_e}\frac{\partial \eta}{\partial t} + \frac{C_B}{R_e^2}\frac{\partial^4\eta}{\partial x^4} - \frac{T_w}{R_e^2}\frac{\partial^2\eta}{\partial x^2} + \frac{k_w}{R_e^2}\eta\right) \\ & \quad = \frac{1}{R_e}\left(\frac{\partial^2 v_z}{\partial r^2} + \frac{1}{r}\frac{\partial v_z}{\partial r} + \frac{\partial^2 v_z}{\partial z^2}\right) + \frac{1}{3R_e}\frac{\partial}{\partial z}\left(\frac{\partial v_r}{\partial r} + \frac{v_r}{r} + \frac{\partial v_z}{\partial z}\right) - \rho\left(\frac{\partial v_z}{\partial t} + v_r\frac{\partial v_z}{\partial r} + v_z\frac{\partial v_z}{\partial z}\right) \\ & \theta = 1 + \eta, \quad \text{at } r = 0 \rightarrow \frac{\partial \theta}{\partial r} = 0 \end{aligned}\right\} \tag{2.9}$$

3 Perturbation analysis

Following the perturbation procedure to introduce the physical properties v_r, v_z, p, θ, and ρ as a mathematical power series with small amplitude ratio "ε" we then substitute it into the governing Eq. (2.8) and their boundary conditions (2.9) to obtain two sets of equations and boundary conditions resulting from collecting the similar power terms of ε and ε^2 which are sufficient for completing the solution. Remarking that the wavy motion results from the elastic wall expansion and contraction and no flow occurs in the absence of this mechanism. The physical properties in power series form are as follows:

$$\left.\begin{aligned} v_r &= \varepsilon u_1(r,z,t) + \varepsilon^2 u_2(r,z,t) + \varepsilon^3 u_3(r,z,t) + \cdots \\ v_z &= \varepsilon v_1(r,z,t) + \varepsilon^2 v_2(r,z,t) + \varepsilon^3 v_3(r,z,t) + \cdots \\ \rho &= 1 + \varepsilon\rho_1(r,z,t) + \varepsilon^2\rho_2(r,z,t) + \varepsilon^3\rho_3(r,z,t) + \cdots \\ \theta &= \theta_0 + \varepsilon\,\theta_1(r,z,t) + \varepsilon^2\theta_2(r,z,t) + \varepsilon^3\theta_3(r,z,t) + \cdots \\ p &= p_0 + \varepsilon p_1(r,z,t) + \varepsilon^2 p_2(r,z,t) + \varepsilon^3 p_3(r,z,t) + \cdots \end{aligned}\right\} \tag{3.1}$$

where θ_o is assumed to be constant.

Applying perturbation methodology, results in the two sets which are indicated as (3.1.1) and (3.1.2) in the appendix section. Also, obtaining two sets for the boundary conditions (2.9) requires expanding Taylor series (3.1.3) about $r = 1$ which are also indicated in appendix section as (3.1.4) and (3.1.5).

Introducing Aarts and Ooms [37] approach to obtain the problem solution, it was chosen in the form

$$\left.\begin{aligned} u_1(r,z,t) &= U_1(r)e^{i\alpha(z-t)} + \overline{U}_1(r)e^{-i\alpha(z-t)} \\ v_1(r,z,t) &= V_1(r)e^{i\alpha(z-t)} + \overline{V}_1(r)e^{-i\alpha(z-t)} \\ p_1(r,z,t) &= P_1(r)e^{i\alpha(z-t)} + \overline{P}_1(r)e^{-i\alpha(z-t)} \\ \rho_1(r,z,t) &= \chi P_1(r)e^{i\alpha(z-t)} + \chi\overline{P}_1(r)e^{-i\alpha(z-t)} \end{aligned}\right\} \tag{3.2}$$

$$\left.\begin{aligned} u_2(r,z,t) &= U_{20}(r) + U_2(r)e^{2i\alpha(x-t)} + \overline{U}_2(r)e^{-2i\alpha(x-t)} \\ v_2(r,z,t) &= V_{20}(r) + V_2(r)e^{2i\alpha(z-t)} + \overline{V}_2(r)e^{-2i\alpha(z-t)} \\ p_2(r,z,t) &= P_{20}(r) + P_2(r)e^{2i\alpha(z-t)} + \overline{P}_2(r)e^{-2i\alpha(z-t)} \\ \rho_2(r,z,t) &= D_{20}(r) + D_2(r)e^{2i\alpha(x-t)} + \overline{D}_2(r)e^{-2i\alpha(z-t)} \end{aligned}\right\} \tag{3.3}$$

Remarking the following:

1- Only 1st-order term in the wall properties boundary condition is sufficient for completing the solution.
2- Sine and cosine are introduced in exponential form.
3- The overbar is the complex variable conjugate.

Substituting relations (3.2) and (3.3) into the sets of "ε and ε^{2}" (3.1.1) and (3.1.2) and their boundary conditions (3.1.4) and (3.1.5), respectively, results in the 1st and 2nd system of equations and their boundary conditions (3.3.1) and (3.3.2) as noted in the appendix section.

Following Eldesoky et al. [42] procedure resulting in the following final form of first and second order solutions, this is well explained in the appendix section.

3.1 First-order solution

$$\left.\begin{aligned} V_1(r) &= C_1 J_3 I_o(\nu r) + C_2 J_2 I_o(\beta r) \\ U_1(r) &= C_1 I_1(\nu r) + C_2 I_1(\beta r) \\ P_1(r) &= C_1 J_4 I_o(\nu r) \\ \theta_1(r) &= C_4 I_o(Ar) \end{aligned}\right\} \tag{3.4a}$$

3.2 Second-order solution

$$\left.\begin{aligned} V_{20}(r) &= D_2 - R_e \int_r^1 \left(V_1(r)\,\overline{U_1}(r) + \overline{V_1}(r) U_1(r) \right) dr \\ U_{20}(r) &= \frac{D_1}{r} - \chi \left(P_1(r)\,\overline{U_1}(r) + \overline{P_1}(r) U_1(r) \right) \\ \theta_{20}(r) &= \int_r^1 \frac{1}{r} \left[\int_r^1 r \left(P_r R_e F_4 - B_r F_5 \right) dr \right] dr \end{aligned}\right\} \quad (3.4b)$$

Also, the net flow rate is represented as [42], noting that $O(\varepsilon^2)$ is sufficient. The relation of axial net flow rate is

$$\langle Q \rangle = 2\pi\,\varepsilon^2 \int_0^1 r\, V_{20}(r,z,t)\, dr \quad (3.5a)$$

After doing integration on (3.5a), it is rewritten in the form

$$\langle Q \rangle = \pi\,\varepsilon^2 \left(D_2 - R_e \int_0^1 r^2 \left(V_1(r)\,\overline{U_1}(r) + \overline{V_1}(r) U_1(r) \right) dr \right) \quad (3.5b)$$

4 Results and discussion

The present work is the first attempt to study the combined influences of wall properties, slip conditions and heat transfer on the peristaltic locomotion of compressible fluid through tube in (r-z) coordinates. Then, to validate the rationality and accuracy of the present work a mathematical comparison for this article is done with Aarts and Ooms [37] and Eldesoky et al. [42] in which the relaxation time effect must be neglected to get the same relation for the net flow rate, net velocity and pressure for compressible flow. It is found that, the main resulting relations for the pressure and velocities and net flux is the same but the difference is obtained from the parameters of interest in the boundary condition, since Aarts and Ooms [37] showed the slip effects and compressibility effects and Eldesoky et al. [42] added to these effects, the influence of relaxation time and in our research we concentrate on the elastic wall properties, slip, compressibility and heat transfer effects.

The following must be noticed:

1. This solution is valid and applicable under the condition $\varepsilon\alpha^2 R_e \ll 1$, mentioned by Takabatake et al. [15].
2. There is absence of wall parameters in this analysis, reducing the mathematical solution of the net flow rate to that resulting from Aarts and Ooms [37].
3. Eldesoky et al. [42] relations can be obtained by neglecting in their article the relaxation time and in this article the wall parameters.

The main principle goal objective of this analysis is to observe the behavior of the fluid transport under the combined qualitative and quantitative characteristics for various emerging physical variables related to the elastic wall, the viscous flow, and the heat transfer. The physical parameters are the flexible wall parameters "$T, D, B,$ and K," the flow parameters "$\chi, \alpha, R_e,$ and Kn," and heat transfer parameter P_r. Expressions for the mean axial velocity, pressure, temperature, and the time averaged flow rate are obtained. The main concert is calculating the net flow rate Q and the temperature. The variation of the net flux Q and temperature distribution under the previous parameters is graphically presented in this section. In order to check the validity for this solution, the condition of [15] stating that $\varepsilon\ \alpha^2 R_e \ll 1$must be verified; therefore the fluid flow is supposed to be laminar and R_e values are taken small. The range of R_e is [0.1:0.3]. Small amplitude ratio is supposed to be $\varepsilon = 0.01$. Also wave number varies in the range within [0 and 1]. The slip flow parameter range is $0 < Kn < 0.15$. If $Kn = 0$ then, nonslip condition is achieved. The liquid compressibility χ is within [0 and 1], in which $\chi = 0$ means incompressible liquid.

In the beginning, Fig. 2 shows the (dimensionless) net flux profiles with the liquid compressibility χ axis for various values of slip parameter "Kn" and elastic wall features "D, T and K," respectively, and its corresponding data in Table 1.

Figure 2a shows that, at constant value for slip parameter $Kn > 0$, when liquid compressibility increases, the net flux decreases and, at $Kn = 0$ nonslip condition, the same trend occurs up to high liquid compressibility $\chi = 0.6$ at which the net flow rate $Q = -1.17473 \times 10^{-5}$, the negative flow rate means that reverse flow begins to occur as nonslip conditions cause attaching the liquid particles to the walls, and then negative velocity appears so that the streamline reverses its direction. Also, for constant value of compressibility number, say $\chi = 0.2$ then by increasing slip coefficient Kn, the net flux increases. It is noticed that, in all cases of slip parameters, maximum flow rate occurs in case of incompressible flow $\chi = 0$. The dissipative factor D effect is presented in Fig. 2b, as it resists the fluid motion and gives the same action of viscosity, where for constant liquid compressibility there is a reduction in the net flow rate against the increase of wall damping factor D. At $D = 200$ and $\chi = 1$the net flow rate has negative value $Q = -1.65 \times 10^{-4}$, which means backward flow takes place

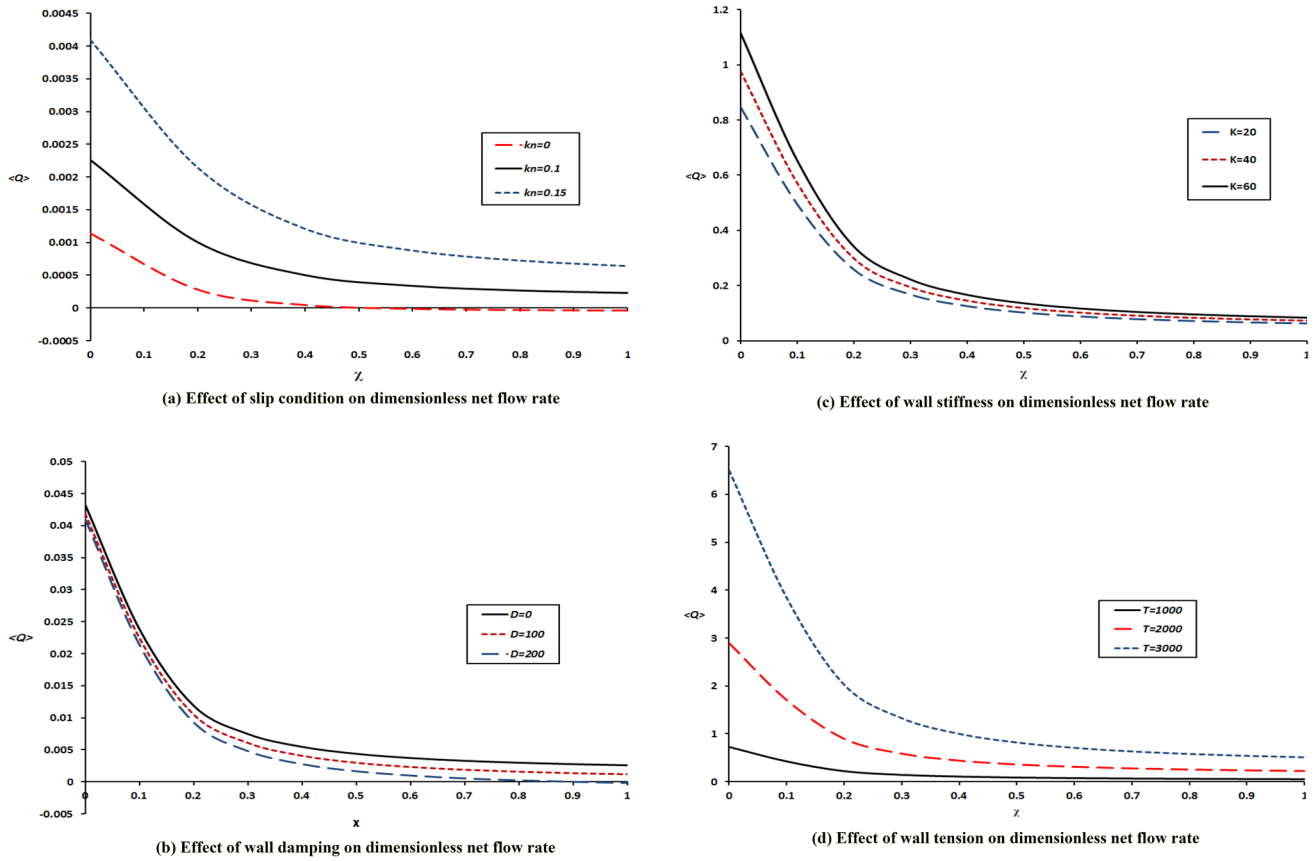

Fig. 2 Variation of dimensionless net flux versus compressibility factor at different values of wall and flow parameters

Table 1 Corresponding to Fig. 2

	a	b	c	d
Wall and flow parameters				
Kn	(0.0–0.1–0.15)	0.15	0.15	0.15
D	0.4	(0.0–100–200)	100	100
K	0.1	10	(20–40–60)	0.1
T	200	200	1000	(1000–2000–3000)
B	20	20	20	20
R_e	0.1	0.1	0.1	0.1
m	0.01	0.01	0.01	0.01
α	0.3	0.5	0.5	0.5

due to this resistive action. It is also noted that at certain value for D, the net flux decreases by increasing χ and maximum flow rates are corresponding to incompressible liquid when $\chi = 0$. Now Fig. 2c illustrates the effect of wall elasticity expressed by spring stiffness K as *Q* increases by increasing K corresponding to fixed value for χ and this effect is obvious up to $\chi = 0.4$, and at $\chi > 0.4$ the net flow rate profiles close to each other. For constant value of wall stiffness *K*, *Q* is inversely proportional with χ. In Fig. 2d wall tension *T* also affects the net flux and gives the same trend for net flux profiles of Fig. 2c but the curves are relatively spaced as there is a proportional relation between *Q* and *T* for constant χ.

Figure 3 shows the net flux profiles versus the wave number α for different values of slip coefficient Kn and viscoelastic wall properties "D, T and K," respectively. The data of Fig. 3 is shown in Table 2.

Slip conditions influence on the flow rate is illustrated in Fig. 3a where for complete slip flow $Kn = 0.15$ the net flux profile changes in proportional relation until reaching its maximum value $Q_{max} = 3,81 \times 10^{-3}$ at $\alpha = 0.65$, and then inversely proportional relation occurs noting that the back flow starts to take place when $\alpha = 0.85$. For certain value of α, increasing *Kn* leads to a rise in *Q*. When $Kn = 0$ (case of nonslip), the back flow early occurs at $\alpha = 0.4$. Damping force affects the net flow rate as shown in Fig. 3b, since it causes a reduction of flow rate resulting in the flow reflux. $D = 0$ reveals that no damping force exists and only vertical movement takes place. Therefore, the net flux is in the stream-wise direction of the pipe up

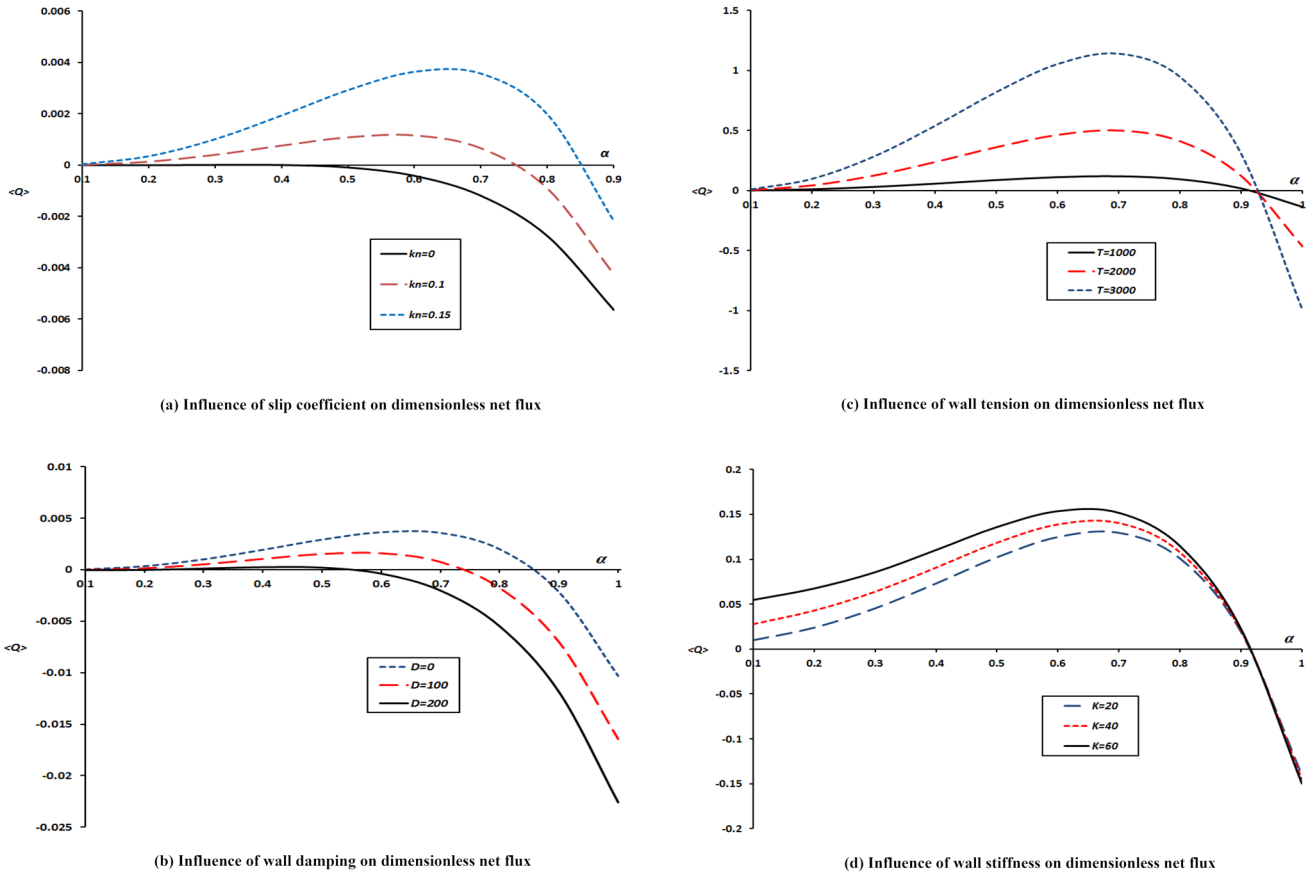

(a) Influence of slip coefficient on dimensionless net flux

(c) Influence of wall tension on dimensionless net flux

(b) Influence of wall damping on dimensionless net flux

(d) Influence of wall stiffness on dimensionless net flux

Fig. 3 Dimensionless net flux distribution against wave number at various values of wall parameters

Table 2 Corresponding to Fig. 3

	a	b	c	d′
Wall and flow parameters				
Kn	(0.0–0.1–0.15)	0.15	0.15	0.15
D	0.4	(0.0–100–200)	100	100
T	200	200	(1000–2000–3000)	1000
K	0.1	0.1	0.1	(20–40–60)
B	20	20	20	20
R_e	0.1	0.1	0.1	0.1
m	0.01	0.01	0.01	0.01
χ	0.5	0.5	0.5	0.5

to $\alpha = 0.88$, before the occurrence of the reverse flow. In addition, for certain value of α the net flux increases up to its maximum value. Then, it is gradually decreasing. Moreover, the effectiveness of wall tension *T* is clear in Fig. 3c. For $T = 3000$ and $T = 2000$, there is a growth in the net flux up to $\alpha = 0.7$ and then the net flux falls off with α but, for $T = 1000$, this trend is slightly sensible. *T* boosts the net flow rate. Q_{max} (for all cases) occurs at $\alpha = 0.7$ and also the back flow starts to exist at $\alpha = 0.92$ after which increasing *T*, increases the back flow. It is visible in Fig. 3d that there is a raise in the net flow rate by increasing wall elasticity *K* and α. But after $\alpha = 0.68$, *Q* reduces until $\alpha = 0.91$at which the back flow exists. It is apparent that *K* effect seems to be similar for higher values of $\alpha > 0.75$.

Figure 4 shows the variation of the net flow rate against different parameters of slip coefficient *Kn*, wall tension *T*, and wall elasticity *K* and the corresponding data is tabulated in Table 3.

The net flux rises by increasing the slip factor *Kn* and the increase in liquid compressibility χ reduces the net flux. When $\chi = 0$ (incompressible liquid), largest profile occurs and, at $Kn = 0.15$, the maximum flow rate appears for all cases of χ, as shown in Fig. 4a. In contrast, as shown in Fig. 4b, for nonslip condition $Kn = 0$ and at $Kn = 0.1$ (slip flow), the back flow is visible and there is an inversely proportional relation of *Q* with *T*, as the net flow falls off and the back flow rises, but, at $Kn = 0.15$ (fully slip flow), there is a proportional relation between *T* and *Q*, and the back flow appears and its amount decreases up to $T = 420$; then it vanishes and the net flow rate will be positive. The

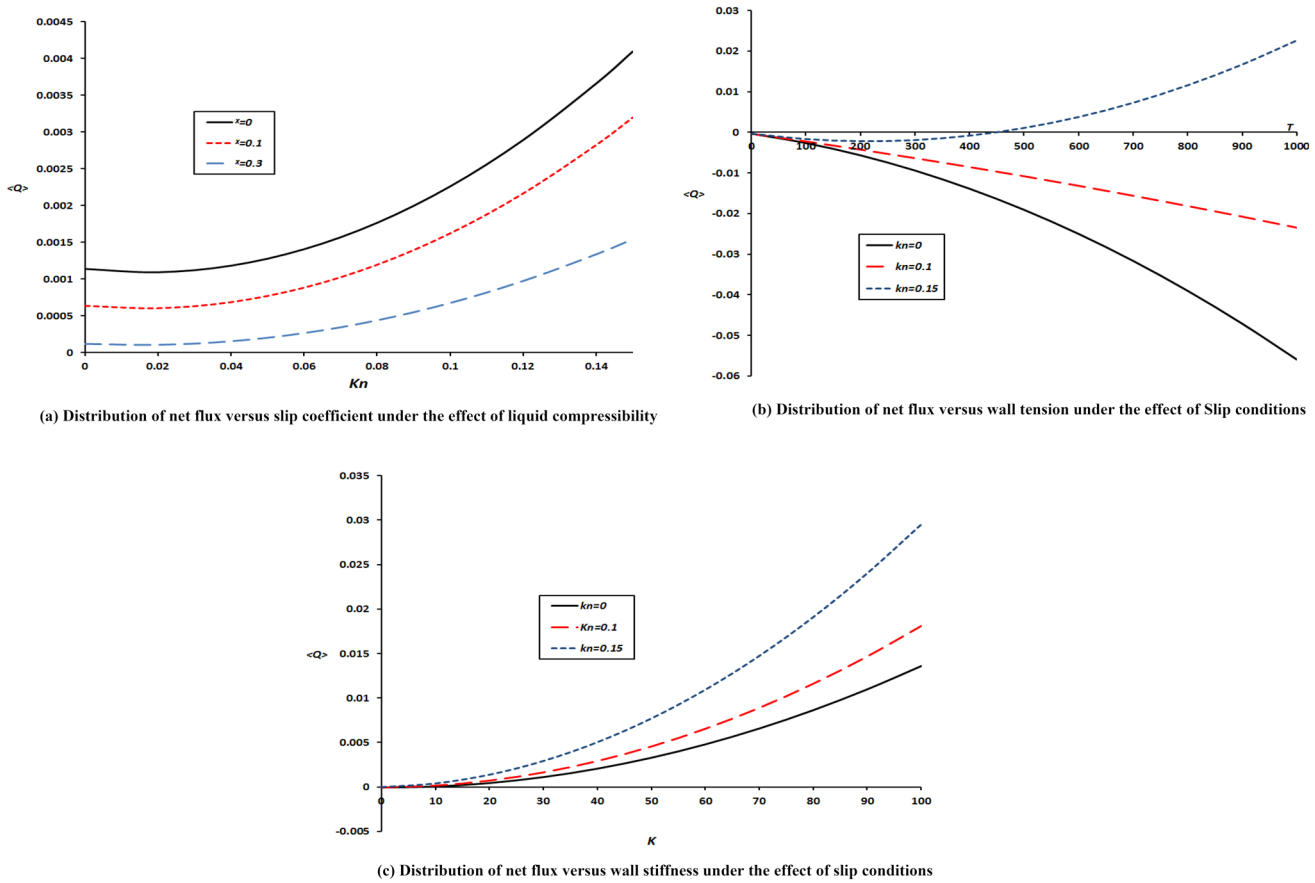

Fig. 4 Effect of flow and wall parameters on the dimensionless net flow rate

maximum flow rate occurs at $T = 1000$ when $Kn = 0.15$ as $Q_{max} = 0.0027$. Increasing in K causes a raise in Q and slip coefficient boosts the net flux as shown in Fig. 4c.

Figure 5 shows the temperature distribution along the pipe against the Prandtl number P_r and slip coefficient Kn, wall tension T, and wall elasticity K.

The temperature decreases across the tube but the increase of $P_r, R_e,$ and α causes increase in the temperature as shown in Figs. 5(a, b, and c), respectively.

Table 3 Corresponding to Fig. 4

	a	b	c
Wall and flow parameters			
χ	(0.0–0.1–0.3)	0.5	0.5
D	0.4	0.1	0.5
K	0.1	0.5	x-axis
T	200	x-axis	20
B	20	20	2
R_e	0.1	0.1	0.2
m	0.01	0.01	0.01
α	0.5	0.9	0.5
Kn	x-axis	(0.0–0.1–0.15)	(0.0–0.1–0.15)

5 Conclusion

This work is related to the peristaltic action through the tube and the fluid flow behavior is studied under the effectiveness of several flow and wall features in the presence of heat transfer. The flow parameters are Reynolds number R_e, compressibility parameter χ, and wave number α. The wall parameters are associated with the elastic wall features and symbolized as D, T, K and B. The heat transfer coefficient is presented as P_r. Net flux profiles Q against χ, α, Kn, T and K are plotted under the effect of the pervious parameters. The temperature distribution is also indicated. The results disclose that, the compressibility factor has a strong impact on the net flux as Q is reduced by rising χ and also, the slip condition seems clearly affecting the net flow as slip factor Kn boosts the net flow rate and the highest net flux takes place at $Kn = 0.15$ (fully slip flow. The parameter of interest is the wall properties and their influences is strongly affect the flow rate behaviour, where, the increase in wall $_d$amping factor D reduces the net flux (resisting the flow) which results in the appearance of the back flow but increasing wall stiffness K and wall tension T results in the growth in the net flux but T

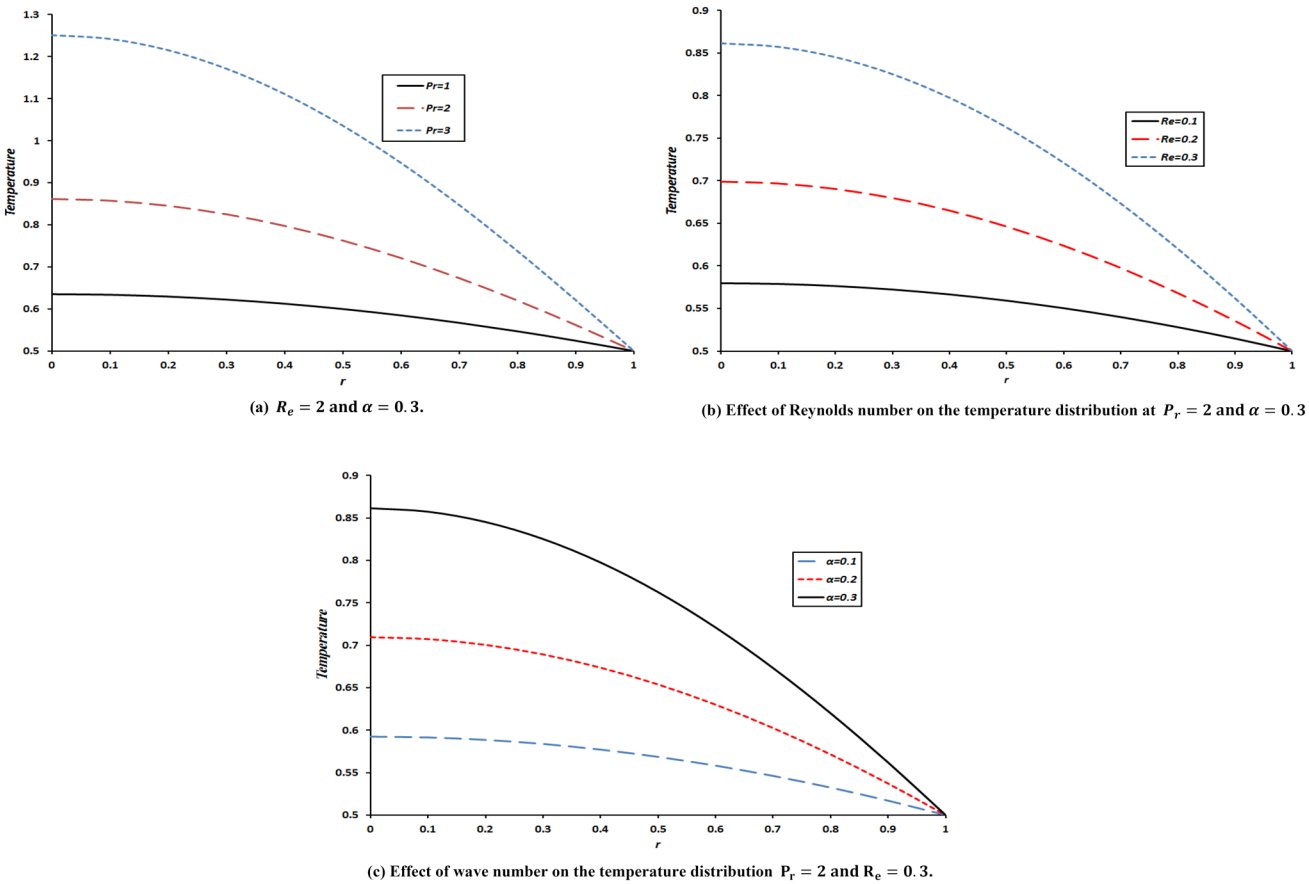

(a) $R_e = 2$ and $\alpha = 0.3$.

(b) Effect of Reynolds number on the temperature distribution at $P_r = 2$ and $\alpha = 0.3$

(c) Effect of wave number on the temperature distribution $P_r = 2$ and $R_e = 0.3$.

Fig. 5 Temperature distribution across the tube

effect is clearer than the profiles of K. The net flux profile varies with the wave number α in proportional relation up to a certain value of α and the backward flow may exist at higher values of wave number. The temperature distribution is increasing by increasing $P_r, R_e,$ and α.

Compliance with ethical standards

Conflict of interest The authors declare that they have no conflict of interest.

Appendix 1: Derivations of equations

The viscous dissipation rate term in Energy equation is given by

$$\Phi = 2\mu\left[\left(\frac{\partial v_r}{\partial r}\right)^2 + \left(\frac{v_r}{r}\right)^2 + \left(\frac{\partial v_z}{\partial z}\right)^2\right] - \frac{2}{3}\mu\left[\frac{\partial v_r}{\partial r} + \frac{v_r}{r} + \frac{\partial v_z}{\partial z}\right]^2 \tag{2.1.1a}$$

$$\vec{V} = v_r\,\hat{e}_r + v_z\,\hat{e}_z \tag{2.1.1b}$$

The dimensionless parameters are

$$\left.\begin{aligned} &\bar{z} = \frac{z}{R},\ \bar{r} = \frac{r}{R},\ \bar{\eta} = \frac{\eta}{R},\ \overline{v_r} = \frac{v_r}{c},\ \overline{v_z} = \frac{v_z}{c},\ \bar{t} = \frac{t\,c}{R},\ \bar{\rho} = \frac{\rho}{\rho_o},\ \bar{p} = \frac{p}{\rho_o c^2},\ \overline{p_o} = \frac{p_o}{\rho_o c^2} \\ &\bar{\theta} = \frac{T - T_o}{T_1 - T_o},\ \bar{T} = \frac{T}{\rho_o v_o^2},\ \overline{m} = \frac{m}{\rho_o R},\ \overline{D} = \frac{D}{\rho_o v_o},\ \overline{B} = \frac{B}{\rho_o R v_o^2},\ \overline{K} = \frac{K R^3}{\rho_o v_o^2} \end{aligned}\right\} \tag{2.7.1a}$$

The dimensionless physical parameters are

$$\left.\begin{aligned} &R_e = \frac{c\rho_0 R}{\mu},\ \upsilon_o = \frac{\mu}{\rho_o},\ \alpha = \frac{2\pi d}{\lambda},\ \varepsilon = \frac{a}{d},\ Kn = \frac{A}{d},\ P_r = \frac{\mu\, c_p}{K_t} \\ &E = \frac{c^2}{c_p(T_1 - T_o)},\ B_r = P_r E,\ \chi = k^* \rho_o\, c^2 \end{aligned}\right\} \tag{2.7.1b}$$

The two sets resulting from the substitution of perturbation series (3.1) into the governing Eq. (2.8) are introduced as following:

The set of ε is

$$\left.\begin{aligned} &\frac{\partial \rho_1}{\partial t} + \frac{\partial u_1}{\partial r} + \frac{u_1}{r} + \frac{\partial v_1}{\partial z} = 0 \\ &\frac{\partial u_1}{\partial t} = \frac{\partial p_1}{\partial r} + \frac{1}{R_e}\left(\frac{\partial^2 u_1}{\partial r^2} + \frac{1}{r}\frac{\partial u_1}{\partial r} - \frac{u_1}{r^2} + \frac{\partial^2 u_1}{\partial z^2}\right) + \frac{1}{3R_e}\frac{\partial}{\partial r}\left(\frac{\partial u_1}{\partial r} + \frac{u_1}{r} + \frac{\partial v_1}{\partial z}\right) \\ &\frac{\partial v_1}{\partial t} = \frac{\partial p_1}{\partial z} + \frac{1}{R_e}\left(\frac{\partial^2 v_1}{\partial r^2} + \frac{1}{r}\frac{\partial v_1}{\partial r} + \frac{\partial^2 v_1}{\partial z^2}\right) + \frac{1}{3R_e}\frac{\partial}{\partial z}\left(\frac{\partial u_1}{\partial r} + \frac{u_1}{r} + \frac{\partial v_1}{\partial z}\right) \\ &P_r R_e \frac{\partial \theta_1}{\partial t} = \frac{\partial^2 \theta_1}{\partial r^2} + \frac{\partial^2 \theta_1}{\partial z^2} + \frac{1}{r}\frac{\partial \theta_1}{\partial r} \end{aligned}\right\} \tag{3.1.1}$$

Taylor series expansion is introduced as following

$$\left.\begin{aligned} v_r(r,\eta,t) &= v_r(1,z,t) + \eta(z,t)\frac{\partial v_r(1,z,t)}{\partial r} + \frac{\eta^2(z,t)}{2}\frac{\partial^2 v_r(1,z,t)}{\partial r^2} + \cdots \\ v_z(r,\eta,t) &= v_z(1,z,t) + \eta(z,t)\frac{\partial v_z(1,z,t)}{\partial r} + \frac{\eta^2(z,t)}{2}\frac{\partial^2 v_z(1,z,t)}{\partial r^2} + \cdots \\ \theta(r,\eta,t) &= \theta(1,z,t) + \eta(z,t)\frac{\partial \theta(1,z,t)}{\partial r} + \frac{\eta^2(z,t)}{2}\frac{\partial^2 \theta(1,z,t)}{\partial r^2} + \cdots \end{aligned}\right\} \tag{3.1.3}$$

The boundary equations resulting from the substitution of perturbation method (3.1) and Taylor series (3.1.3) into the boundary conditions (2.9) are introduced in the form of two sets as following:

The set of ε is

$$\left.\begin{aligned} &u_1(1,z,t) = -\frac{i\alpha}{2}\left(e^{i\alpha(z-t)} - e^{-i\alpha(z-t)}\right), \quad v_1(1,z,t) = Kn\frac{\partial v_1(1,z,t)}{\partial r} \\ &\theta_1(1,z,t) = \frac{1}{2}\left(e^{i\alpha(z-t)} + e^{-i\alpha(z-t)}\right), \quad \frac{\partial \theta_1(0,z,t)}{\partial r} = 0 \\ &\frac{1}{R_e}\left(\frac{\partial^2 v_1(1,z,t)}{\partial r^2} + \frac{1}{r}\frac{\partial v_1(1,z,t)}{\partial r} + \frac{\partial^2 v_1(1,z,t)}{\partial z^2}\right) + \frac{1}{3R_e}\frac{\partial}{\partial z}\left(\frac{\partial u_1(1,z,t)}{\partial r} + \frac{u_1(1,z,t)}{r} + \frac{\partial v_1(1,z,t)}{\partial z}\right) \\ &\quad - \frac{\partial v_1(1,z,t)}{\partial t} = -\frac{i\delta_a}{2}\left(e^{i\alpha(z-t)} - e^{-i\alpha(z-t)}\right) + \frac{\delta_b}{2}\left(e^{i\alpha(z-t)} + e^{-i\alpha(z-t)}\right) \end{aligned}\right\} \tag{3.1.4}$$

The set of ε^2 is

$$\left.\begin{aligned} &\frac{\partial \rho_2}{\partial t} + u_1\frac{\partial \rho_1}{\partial r} + v_1\frac{\partial \rho_1}{\partial z} + \frac{\partial u_2}{\partial r} + \frac{u_2}{r} + \frac{\partial v_2}{\partial z} + \rho_1\left(\frac{\partial u_1}{\partial r} + \frac{u_1}{r} + \frac{\partial v_1}{\partial z}\right) = 0 \\ &\frac{\partial u_2}{\partial t} + \rho_1\frac{\partial u_1}{\partial t} + u_1\frac{\partial u_1}{\partial r} + v_1\frac{\partial u_1}{\partial z} = -\frac{\partial p_2}{\partial r} + \frac{1}{R_e}\left[\frac{\partial^2 u_2}{\partial r^2} + \frac{1}{r}\frac{\partial u_2}{\partial r} - \frac{u_2}{r^2} + \frac{\partial^2 u_2}{\partial z^2}\right] + \frac{1}{3R_e}\frac{\partial}{\partial r}\left(\frac{\partial u_2}{\partial r} + \frac{u_2}{r} + \frac{\partial v_2}{\partial z}\right) \\ &\frac{\partial v_2}{\partial t} + \rho_1\frac{\partial v_1}{\partial t} + u_1\frac{\partial v_1}{\partial r} + v_1\frac{\partial v_1}{\partial z} = -\frac{\partial p_2}{\partial z} + \frac{1}{R_e}\left[\frac{\partial^2 v_2}{\partial r^2} + \frac{1}{r}\frac{\partial v_2}{\partial r} + \frac{\partial^2 v_2}{\partial z^2}\right] + \frac{1}{3R_e}\frac{\partial}{\partial z}\left(\frac{\partial u_2}{\partial r} + \frac{u_2}{r} + \frac{\partial v_2}{\partial z}\right) \end{aligned}\right\} \tag{3.1.2a}$$

$$\left.\begin{aligned} &P_r R_e\left(\frac{\partial \theta_2}{\partial t} + \rho_1\frac{\partial \theta_1}{\partial t} + u_1\frac{\partial \theta_1}{\partial r} + v_1\frac{\partial \theta_1}{\partial z}\right) = \left(\frac{\partial^2 \theta_2}{\partial r^2} + \frac{1}{r}\frac{\partial \theta_2}{\partial r} + \frac{\partial^2 \theta_2}{\partial z^2}\right) + 2B_r\left[\left(\frac{\partial u_1}{\partial r}\right)^2 + \left(\frac{u_1}{r}\right)^2 + \left(\frac{\partial v_1}{\partial r}\right)^2\right] \\ &\quad - \frac{2}{3}B_r\left[\left(\frac{\partial u_1}{\partial r}\right)^2 + 2\left(\frac{\partial u_1}{\partial r}\right)\left(\frac{\partial v_1}{\partial z}\right) + \frac{2u_1}{r}\left(\frac{\partial u_1}{\partial r}\right) + \left(\frac{\partial u_1}{\partial z} + \frac{\partial v_1}{\partial z}\right)^2 + \left(\frac{u_1}{r}\right)^2 + \left(\frac{\partial v_1}{\partial z}\right)^2\right] \\ &\quad + B_r\left[\left(\frac{\partial v_1}{\partial z}\right)^2 + \left(\frac{\partial u_1}{\partial z}\right)^2 + 2\left(\frac{\partial u_1}{\partial z}\right)\left(\frac{\partial v_1}{\partial z}\right)\right] \end{aligned}\right\} \tag{3.1.2b}$$

The set of ε^2 is

$$\left.\begin{aligned} &v_2(1,z,t)+\frac{1}{2}\left(e^{i\alpha(z-t)}+e^{-i\alpha(z-t)}\right)\frac{\partial v_1(1,z,t)}{\partial r}=Kn\left(\frac{\partial v_2(1,z,t)}{\partial r}-\frac{1}{2}\left(e^{i\alpha(z-t)}+e^{-i\alpha(z-t)}\right)\frac{\partial^2 v_1(1,z,t)}{\partial r^2}\right)\\ &u_2(1,z,t)+\frac{1}{2}\left(e^{i\alpha(z-t)}+e^{-i\alpha(z-t)}\right)\frac{\partial u_1(1,z,t)}{\partial r}=0,\\ &\theta_2(1,z,t)+\frac{1}{2}\left(e^{i\alpha(z-t)}+e^{-i\alpha(z-t)}\right)\frac{\partial \theta_1(1,z,t)}{\partial r}=0\\ &\frac{\partial\theta_2(0,z,t)}{\partial r}=0 \end{aligned}\right\} \quad (3.1.5)$$

The following equations are introducing the 1st and 2nd system of equations and their boundary conditions resulting from the substitution of Eqs. (3.2) and (3.3) into the two sets Eqs. (3.1.1), (3.1.2) and their boundary conditions (3.1.4) and (3.1.5).

First-order system

$$U_1'+\frac{U_1}{r}+i\alpha V_1-i\alpha\chi P_1=0 \quad (3.3.1a)$$

$$-i\alpha U_1=-P_1'+\frac{1}{R_e}\left(U_1''+\frac{U_1'}{r}-\frac{U_1}{r^2}-\alpha^2U_1\right)+\frac{1}{3R_e}\frac{d}{dr}\left[U_1'+\frac{U_1}{r}+i\alpha V_1\right] \quad (3.3.1b)$$

$$-i\alpha V_1=-i\alpha P_1+\frac{1}{R_e}\left(V_1''+\frac{V_1'}{r}-\alpha^2V_1\right)+\frac{i\alpha}{3R_e}\left[U_1'+\frac{U_1}{r}+i\alpha V_1\right] \quad (3.3.1c)$$

$$\theta_1''+\frac{1}{r}\theta_1'-\left(\alpha^2-i\alpha R_eP_r\right)\theta_1=0 \quad (3.3.1d)$$

Second-order system

$$-P_{20}'+\frac{4}{3R_e}\left(U_{20}''+\frac{U_{20}'}{r}-\frac{U_{20}}{r^2}\right)=F_1 \quad (3.3.2a)$$

$$V_{20}''+\frac{V_{20}'}{r}=R_eF_2 \quad (3.3.2b)$$

$$U_{20}'+\frac{U_{20}}{r}=-\chi F_3 \quad (3.3.2c)$$

$$D_{20}=\chi P_{20}+\chi P_1\overline{P_1} \quad (3.3.2d)$$

$$\theta_{20}''+\frac{\theta_{20}'}{r}=P_rR_eF_4-B_rF_5 \quad (3.3.2e)$$

First-order boundary conditions

$$V_1(1)=Kn\,V_1'(1) \quad (3.3.3a)$$

$$U_1(1)=\frac{-i\,\alpha}{2} \quad (3.3.3b)$$

$$V_1''(1)+V_1'(1)+\left(i\alpha R_e-\frac{4}{3}\alpha^2\right)V_1(1)+\frac{i\alpha}{3}\left(U_1'(1)+U_1(1)\right)=R_e\delta \quad (3.3.3c)$$

$$\theta_1(1)=\frac{1}{2} \quad (3.3.3d)$$

$$\theta_1'(0)=0 \quad (3.3.3e)$$

Second-order boundary conditions

$$U_{20}(1)+\frac{1}{2}\left[U_1'(1)+\overline{U_1}'(1)\right]=0 \quad (3.3.4a)$$

$$V_{20}(1)+\frac{1}{2}\left[V_1'(1)+\overline{V_1}'(1)\right]=Kn\left[V_{20}(1)'+\frac{1}{2}\left(\overline{V_1}''(1)+V_1''(1)\right)\right] \quad (3.3.4b)$$

$$\theta_{20}(1)+\frac{1}{2}\left[\theta_1'(1)+\overline{\theta_1}'(1)\right]=0 \quad (3.3.4c)$$

$$\theta_{20}'(0)=0 \quad (3.3.4e)$$

such that

$$F_1=\left[i\alpha\chi\left(P_1\overline{U_1}+\overline{P_1}U_1\right)+i\alpha\left(U_1\overline{V_1}-\overline{U_1}V_1\right)+U_1\overline{U_1}'+\overline{U_1}U_1'\right] \quad (3.3.5a)$$

$$F_2=\left[i\alpha\chi\left(P_1\overline{V_1}-\overline{P_1}V_1\right)+U_1\overline{V_1}'+\overline{U_1}V_1'\right] \quad (3.3.5b)$$

$$F_3=\left[P_1\,\overline{U_1}'+\overline{P_1}\,U_1'+\frac{1}{r}\left(P_1\,\overline{U_1}+\overline{P_1}\,U_1\right)+U_1\overline{P_1}'+\overline{U_1}P_1'\right] \quad (3.3.5c)$$

$$F_4=\left[P_1\overline{\theta_1}'+\overline{U_1}\theta_1'+i\alpha\left(\theta_1\overline{V_1}-\overline{\theta_1}V_1\right)+i\alpha\chi\left(P_1\overline{\theta_1}-\overline{P_1}\theta_1\right)\right] \quad (3.3.5d)$$

$$F_5 = \left[\frac{8}{3}U_1'\overline{U_1'} + \left(2\alpha^2 - \frac{8}{3r^2}\right)\overline{U_1}\,U_1 + +\frac{14\alpha^2}{3}\overline{V_1}\,V_1 + \left(2\alpha^2 + \frac{4i\alpha}{3r}\right)\overline{V_1}U_1 + \left(2\alpha^2 - \frac{4i\alpha}{3r}\right)\overline{U_1}V_1 - \frac{4}{3r}\left(\overline{U_1}'U_1 + \overline{U_1}U_1'\right) + \frac{4i\alpha}{3}\left(\overline{V_1}U_1' - V_1\overline{U_1}'\right)\right] \tag{3.3.5e}$$

According to the solution procedure of Eldesoky et al. [42] results in the solution of (3.3.1) and (3.3.2) under their boundary conditions (3.3.3–3.3.4). Substituting (3.3.1a) into (3.3.1b) and (3.3.1c) results in the following relations:

$$-\gamma P_1' + \left(U_1'' + \frac{U_1'}{r} - \frac{U_1}{r^2} - \beta^2 U_1\right) = 0 \tag{3.3.6a}$$

$$-\gamma P_1 - \frac{i}{\alpha}\left(V_1'' + \frac{V_1'}{r} - \beta^2 V_1\right) = 0 \tag{3.3.6b}$$

Using Eq. (3.3.1a) to remove V_1 term and its derivatives from Eq. (3.3.6b) and obtain the following equation.

$$\frac{-i\chi}{\alpha}\left(P_1'' + \frac{P_1'}{r} - \left(\beta^2 + \frac{i\alpha\gamma}{\chi}\right)P_1\right) + \frac{1}{\alpha^2}\left(\frac{d}{dr} + \frac{1}{r}\right)\left(U_1'' + \frac{U_1'}{r} - \frac{U_1}{r^2} - \beta^2 U_1\right) = 0 \tag{3.3.6c}$$

Differentiate Eq. (3.3.6c) with respect to r and using Eq. (3.3.6a) to eliminate P_1 and its derivatives then Eq. (3.3.6c) are rewritten as follows.

$$\left[\frac{-i\chi}{\alpha\gamma}\left(\frac{d^2}{dr^2} + \frac{1}{r}\frac{d}{dr} - \frac{1}{r^2} - \left(\beta^2 + \frac{i\alpha\gamma}{\chi}\right)_1\right) + \frac{1}{\alpha^2}\left(\frac{d^2}{dr^2} + \frac{1}{r}\frac{d}{dr} - \frac{1}{r^2}\right)\right]\left(U_1'' + \frac{U_1'}{r} - \frac{U_1}{r^2} - \beta^2 U_1\right) = 0 \tag{3.3.6d}$$

Multiplying Eq. (3.3.6d) with α^2 resulting in:

$$B\left(\frac{d^2}{dr^2} + \frac{1}{r}\frac{d}{dr} - \frac{1}{r^2} - \nu^2\right)\left(\frac{d^2}{dr^2} + \frac{1}{r}\frac{d}{dr} - \frac{1}{r^2} - \beta^2\right)U_1 = 0 \tag{3.3.6e}$$

Solving (3.3.6e) as it seems to be modified Bessel differential equation results in

$$U_1(r) = C_1 I_1(\nu r) + C_2 I_1(\beta r) \tag{3.3.7a}$$

Substituting (3.3.7a) into (3.3.6a) and then integrating the resulting equation to obtain relation of pressure, one has

$$P_1(r) = \frac{C_1(\nu^2 - \beta^2)}{\nu\gamma} I_o(\nu r) + C_3 \tag{3.3.7b}$$

In order to get expression for V_1 velocity, substitute (3.3.7a) and (3.3.7b) into (3.3.1a) resulting in

$$V_1(r) = C_1 J_1 I_o(\nu r) + C_2 J_2 I_o(\beta r) + \chi C_3 \tag{3.3.7c}$$

Solving (3.3.1d) results in

$$\theta_1(r) = C_4 I_o(A r) \tag{3.3.7d}$$

Using (3.3.6b) to get relation for C_3 in terms of C_1 and then substituting into (3.3.7b) and (3.3.7c) and rewriting the 1st-order velocity and pressure expressions in the final form as follows, one has

$$V_1(r) = C_1 J_3 I_o(\nu r) + C_2 J_2 I_o(\beta r) \tag{3.3.7f}$$

$$P_1(r) = C_1 J_4 I_o(\nu r) \tag{3.3.7g}$$

Noting that $U_1(r), V_1(r), P_1(r),$ and$\theta_1(r)$ are singular at $r = 0$ and then terms of modified Bessel function of second kind are neglected.

Solution of the 2nd-order system (3.3.2) under their boundary conditions (3.3.4) results in relations for the second-order velocities, pressure, and temperature as follows.

Equation (3.3.5c) is rewritten in the differential form.

$$F_3 = \frac{1}{r}\frac{d}{dr}\left[r\left(P_1\overline{U_1} + \overline{P_1}U_1\right)\right] \tag{3.3.8a}$$

Then, (3.3.2c) is a linear ordinary differential equation and its solution is given by

$$U_{20}(r) = \frac{D_1}{r} - \chi\left(P_1(r)\overline{U_1}(r) + \overline{P_1}(r)U_1(r)\right) \tag{3.3.8b}$$

Obtaining D_1 requires equating $U_1'(r)$ relation (3.3.1a) and its conjugate with $U_{20}(r)$ relation (3.3.8b) at r = 1 in the boundary condition (3.3.4a) in the existence of relations (3.3.3a) and (3.3.3b) for $V_1(1)$ and $U_1(1)$, respectively, and their conjugates therefore.

$$D_1 = \frac{i\alpha}{2}Kn\left(V_1'(1) - \overline{V_1'}(1)\right) \tag{3.3.8c}$$

If $Kn = 0$ then $D_1 = 0$ as Aarts and Ooms [37].

Rewriting (3.3.5b) in the differential form requires removing P_1 from Eq. (3.3.5c) using Eq. (3.3.1a) and then it is obtained as

$$F_2 = \frac{1}{r}\frac{d}{dr}\left[r\left(V_1\,\overline{U_1} + \overline{V_1}\,U_1\right)\right] \tag{3.3.8d}$$

Multiplying (3.3.2b) with r and then integrating it two times results in the general solution for $V_{20}(r)$.

It is noticed that $V_{20}(r)$ is singular at $r = 0$.

$$V_{20}(r) = D_2 - R_e \int_r^1 \left(V_1(r)\,\overline{U_1}(r) + \overline{V_1}(r)U_1(r)\right) dr \tag{3.3.8e}$$

The constant D_2 can be obtained with the aid of boundary condition (3.3.4b) as follows:

$$D_2 = Kn\left[V_{20}'(1) + \frac{1}{2}\left(\overline{V_1}''(1) + V_1''(1)\right)\right] - \frac{1}{2}\left[V_1'(1) + \overline{V_1}'(1)\right] \tag{3.3.8f}$$

Now, the relation for the 2nd-order temperature $\theta_{20}(r)$ is obtained as a result of multiplying (3.3.2e) with r and then integrating the resulting equation with respect to r two times.

$$\theta_{20}(r) = \int_r^1 \frac{1}{r}\left[\int_r^1 r\left(P_r R_e F_4 - B_r F_5\right) dr\right] dr \tag{3.3.8g}$$

The time average flow rate along one period of time is suitable for calculating the net flow rate.

since the net available velocity is

$$\langle V_z \rangle = \varepsilon^2 V_{20}(r) \tag{3.3.9}$$

Appendix 2: Constants

In this section, the constants mentioned in the previous equations are introduced as following:

The constants in Eq. (3.1.4) are

$$\left.\begin{aligned} \delta_a &= m\alpha^3 - \frac{B\alpha^5}{R_e^2} - \frac{T\alpha^3}{R_e^2} - \frac{K\alpha}{R_e^2} \\ \delta_b &= \frac{D\alpha^2}{R} \end{aligned}\right\} \tag{3.6a}$$

The constant in Eq. (3.3.3c) is

$$\delta = \frac{-i\alpha}{2R_e^2}\left[iD\alpha R_e - \alpha^2 R_e^2 m - B\alpha^4 - T\alpha^2 - K\right] \tag{3.6b}$$

The constants in Eqs. (3.3.6a) and (3.3.6e) are

$$\left.\begin{aligned} \beta &= \sqrt{\alpha^2 - i\alpha R_e} \\ \gamma &= R_e - \frac{i\alpha\chi}{3} \\ B &= 1 - \frac{i\alpha\chi}{\gamma} \\ \upsilon^2 &= \beta^2 - \frac{\beta^2 - \alpha^2}{B} \end{aligned}\right\} \tag{3.6c}$$

The constants mentioned in the equations of (3.3.7) are

$$J_1 = \frac{\chi(\nu^2 - \beta^2)}{\nu\,\gamma} + \frac{i\,\nu}{\alpha},\quad J_2 = \frac{i\,\beta}{\alpha},\quad J_3 = J_1 + \frac{\chi R_1}{R_2},\quad J_4 = \frac{(\nu^2 - \beta^2)}{\nu\,\gamma} + \frac{R_1}{R_2},\quad J_5 = i\alpha R_e - \frac{4}{3}\alpha^2,\quad J_6 = \frac{i\alpha}{3} \tag{3.6d}$$

$$R_1 = -\left(\frac{\nu^2 - \beta^2}{\nu}\right)\left(1 + \frac{i\nu J_1}{\alpha}\right),\quad R_2 = \gamma - \frac{i\beta^2\chi}{\alpha},\quad R_3 = \frac{Kn\,J_2\,\beta\,I_1(\beta) - J_2 I_o(\beta)}{J_3 I_o(\nu) - Kn\,J_3\,\nu\,I_1(\nu)} \tag{3.6e}$$

$$R_4 = \frac{R_e\,\delta}{\left(J_3\nu^2 + J_3 J_5 + J_6\nu\right)I_o(\nu)},\quad R_5 = \frac{\left(J_2\beta^2 + J_2 J_5 + J_6\beta\right)I_o(\beta)}{\left(J_3\nu^2 + J_3 J_5 + J_6\nu\right)I_o(\nu)},\quad A = \sqrt{\alpha^2 - i\,\alpha\,R_e\,P_r} \tag{3.6f}$$

$$C_1 = \frac{R_3 R_4}{R_3 + R_5},\quad C_2 = \frac{R_4}{R_3 + R_5},\quad C_3 = \frac{C_1 R_1 I_o(\nu\,r)}{R_1},\quad C_4 = \frac{1}{2\,I_o(A)} \tag{3.6g}$$

The functions of Eq. (3.3.8f) are

$$\left.\begin{aligned} V_1'(1) &= C_1 J_3 \nu I_1(\nu) + C_2 J_2 \beta I_1(\beta) \\ V_1''(1) &= C_1 J_3 \nu^2 I_o(\nu) - C_1 J_3 \nu I_1(\nu) + C_2 J_2 \beta^2 I_o(\beta) - C_2 J_2 \beta I_1(\beta) \\ V_{20}'(1) &= R_e\left[V_1(1)\,\overline{U_1}(1) + \overline{V_1}(1)U_1(1)\right] \end{aligned}\right\} \tag{3.6h}$$

References

1. Latham TW (1966) Fluid motions in a peristaltic pump. Massachusetts Institute of Technology, Cambridge
2. Burns J, Parkes T (1967) Peristaltic motion. J Fluid Mech 29(4):731–743

3. Shapiro AH (1967) Pumping and retrograde diffusion in peristaltic waves. In: Proceedings of the workshop in ureteral reflux in children, Washington, DC, 1967, pp 109–126
4. Shapiro AH, Jaffrin MY, Weinberg SL (1969) Peristaltic pumping with long wavelengths at low Reynolds number. J Fluid Mech 37(4):799–825
5. Fung Y, Yih C (1968) Peristaltic transport. J Appl Mech 35(4):669–675
6. Srivastava L, Srivastava V (1982) Peristaltic transport of a two-layered model of physiological fluid. J Biomech 15(4):257–265
7. Srivastava L, Srivastava V (1984) Peristaltic transport of blood: casson model—II. J Biomech 17(11):821–829
8. Srivastava L, Srivastava V (1985) Peristaltic transport of a non-Newtonian fluid: applications to the vas deferens and small intestine. Ann Biomed Eng 13(2):137–153
9. Srivastava L, Srivastava V (1988) Peristaltic transport of a power-law fluid: application to the ductus efferentes of the reproductive tract. Rheol Acta 27(4):428–433
10. Hina S, Mustafa M, Hayat T, Alotaibi ND (2015) On peristaltic motion of pseudoplastic fluid in a curved channel with heat/mass transfer and wall properties. Appl Math Comput 263:378–391
11. Hina S, Mustafa M, Hayat T, Alsaedi A (2016) Peristaltic transport of Powell-Eyring fluid in a curved channel with heat/mass transfer and wall properties. Int J Heat Mass Transf 101:156–165
12. Makinde O, Reddy MG, Reddy KV (2017) Effects of thermal radiation on MHD peristaltic motion of walters-b fluid with heat source and slip conditions. J Appl Fluid Mech 10(4):1105–1112
13. Bhatti M, Zeeshan A (2017) Heat and mass transfer analysis on peristaltic flow of particle–fluid suspension with slip effects. J Mech Med Biol 17(02):1750028
14. Eldesoky IM, Abumandour RM, Abdelwahab ET (2019) Analysis for various effects of relaxation time and wall properties on compressible maxwellian peristaltic slip flow. Z Naturforsch A 74(4):317–331
15. Takabatake S, Ayukawa K, Mori A (1988) Peristaltic pumping in circular cylindrical tubes: a numerical study of fluid transport and its efficiency. J Fluid Mech 193:267–283
16. El-Shehawy E, El-Dabe N, El-Desoky I (2006) Slip effects on the peristaltic flow of a non-Newtonian Maxwellian fluid. Acta Mech 186(1–4):141–159
17. Kamel MH, Eldesoky IM, Maher BM, Abumandour RM (2015) Slip effects on peristaltic transport of a particle–fluid suspension in a planar channel. Appl Bionics Biomech. https://doi.org/10.1155/2015/703574
18. Tang D, Rankin S (1993) Numerical and asymptotic solutions for peristaltic motion of nonlinear viscous flows with elastic free boundaries. SIAM J Sci Comput 14(6):1300–1319
19. Shen M, Ebel D (1987) Asymptotic methods for peristaltic transport of a heat-conducting fluid. J Math Anal Appl 127(1):49–71
20. Dar AA, Elangovan K (2017) Influence of an inclined magnetic field on heat and mass transfer of the peristaltic flow of a couple stress fluid in an inclined channel. World J Eng 14(1):7–18
21. Abd-Alla A, Abo-Dahab S, Kilicman A, El-Semiry R (2014) Effect of heat and mass transfer and rotation on peristaltic flow through a porous medium with compliant walls. Multidiscip Model Mater Struct 10(3):399–415
22. Tang D, Shen M (1993) Nonstationary peristaltic transport of a heat-conducting fluid. J Math Anal Appl 174:265
23. Tanda G, Vittori G (1996) Fluid flow and heat transfer in a two-dimensional wavy channelStrömungsverhalten und Wärmeübergang in einem zweidimesionalen, einseitig gewellten Kanal. Heat Mass Transf 31(6):411–418
24. Srinivas S, Kothandapani M (2008) Peristaltic transport in an asymmetric channel with heat transfer—a note. Int Commun Heat Mass Transfer 35(4):514–522
25. Vajravelu K, Radhakrishnamacharya G, Radhakrishnamurty V (2007) Peristaltic flow and heat transfer in a vertical porous annulus, with long wave approximation. Int J Non-Linear Mech 42(5):754–759
26. Vasudev C, Rao UR, Rao GP, Subba M, Res IJCS (2011) Peristaltic flow of a Newtonian fluid through a porous medium in a vertical tube under the effect of a magnetic field. Int J Curr Sci Res 1(3):105–110
27. Mekheimer KS (2008) The influence of heat transfer and magnetic field on peristaltic transport of a Newtonian fluid in a vertical annulus: application of an endoscope. Phys Lett A 372(10):1657–1665
28. Nadeem S, Akbar NS (2009) Influence of heat transfer on a peristaltic transport of Herschel-Bulkley fluid in a non-uniform inclined tube. Commun Nonlinear Sci Numer Simul 14(12):4100–4113
29. Pandey S, Chaube M (2011) Study of wall properties on peristaltic transport of a couple stress fluid. Meccanica 46(6):1319–1330
30. Hina S, Hayat T, Asghar S, Obaidat S (2012) Peristaltic flow of Maxwell fluid in an asymmetric channel with wall properties. Int J Phys Sci 7(14):2145–2155
31. Radhakrishnamacharya G, Srinivasulu C (2007) Influence of wall properties on peristaltic transport with heat transfer. CR Mec 335(7):369–373
32. Srinivas S, Gayathri R, Kothandapani M (2009) The influence of slip conditions, wall properties and heat transfer on MHD peristaltic transport. Comput Phys Commun 180(11):2115–2122
33. Srinivas S, Kothandapani M (2009) The influence of heat and mass transfer on MHD peristaltic flow through a porous space with compliant walls. Appl Math Comput 213(1):197–208
34. Eldabe NT, Abou-Zeid MY (2010) The wall properties effect on peristaltic transport of micropolar non-Newtonian fluid with heat and mass transfer. Math Probl Eng. https://doi.org/10.1155/2010/898062
35. Hayat T, Hina S, Ali N (2010) Effect of wall properties on the magnetohydrodynamic peristaltic flow of a Maxwell fluid with heat transfer and porous medium. Numer Methods Part Differ Equ 26(5):1099–1114
36. Anderson JD (1990) Modern compressible flow: with historical perspective. McGraw-Hill, New York
37. Aarts A, Ooms G (1998) Net flow of compressible viscous liquids induced by travelling waves in porous media. J Eng Math 34(4):435–450
38. Mekheimer KS, Abdel-Wahab A (2011) Effect of wall compliance on compressible fluid transport induced by a surface acoustic wave in a microchannel. Numer Methods Part Differ Equ 27(3):621–636
39. Eldesoky IM, Abdelsalam S, Abumandour R, Kamel M, Vafai K (2017) Interaction between compressibility and particulate suspension on peristaltically driven flow in planar channel. Appl Math Mech 38(1):137–154
40. Elshehawey E, El-Saman AE-R, El-Shahed M, Dagher M (2005) Peristaltic transport of a compressible viscous liquid through a tapered pore. Appl Math Comput 169(1):526–543
41. Eldesoky IM, Mousa AA (2009) Peristaltic pumping of fluid in cylindrical tube and its applications in the field of aerospace. In: 13th International conference on aerospace sciences and aviation technology, Military Technical College, Cairo, 2009, pp 1–14
42. Eldesoky IM, Mousa A (2010) Peristaltic flow of a compressible non-Newtonian Maxwellian fluid through porous medium in a tube. Int J Biomath 3(02):255–275
43. Eldesoky IM (2012) Influence of slip condition on peristaltic transport of a compressible Maxwell fluid through porous medium in a tube. Int J Appl Math Mech 8(2):99–117
44. Salih A (2011) Conservation equations of fluid dynamics. Department of Aerospace Engineering Indian Institute of Space Science and Technology, Thiruvananthapuram